DYNAMIC RESPONSE OF CONCRETE AND CONCRETE STRUCTURES

FIRST ANNUAL TECHNICAL REPORT

LAWRENCE E. MALVERN

C. ALLEN ROSS

DEPARTMENT OF ENGINEERING SCIENCES

UNIVERSITY OF FLORIDA

GAINESVILLE, FLORIDA 32611

26 January 1984

U.S. AIR FORCE OFFICE OF SCIENTIFIC RESEARCH

CONTRACT NUMBER AFOSR F49620-83-K-0007

UNIVERSITY OF FLORIDA

APPROVED FOR PUBLIC RELEASE; DISTRIBUTION UNLIMITED

UNCLASSIFIED

SECURITY CLASSIFICATION OF THIS PAGE *(When Data Entered)*

REPORT DOCUMENTATION PAGE	READ INSTRUCTIONS BEFORE COMPLETING FORM
1. REPORT NUMBER **AFOSR-TR- 84-0165**	2. GOVT ACCESSION NO. AD-A139194
3. RECIPIENT'S CATALOG NUMBER	
4. TITLE *(and Subtitle)* DYNAMIC RESPONSE OF CONCRETE AND CONCRETE STRUCTURES	5. TYPE OF REPORT & PERIOD COVERED Annual Technical Report 1 DEC 1982 - 30 NOV 1983
	6. PERFORMING ORG. REPORT NUMBER
7. AUTHOR(s) Lawrence E. Malvern C. Allen Ross	8. CONTRACT OR GRANT NUMBER(s) F49620-83-K-0007
9. PERFORMING ORGANIZATION NAME AND ADDRESS Department of Engineering Sciences University of Florida Gainesville, Florida 32611	10. PROGRAM ELEMENT, PROJECT, TASK AREA & WORK UNIT NUMBERS 61102F 2307/C2
11. CONTROLLING OFFICE NAME AND ADDRESS Air Force Office of Scientific Research / NA Directorate of Aerospace Sciences, Bldg. 410 Bolling AFB, D.C. 20332	12. REPORT DATE 26 January 1984 13. NUMBER OF PAGES 50
14. MONITORING AGENCY NAME & ADDRESS *(if different from Controlling Office)*	15. SECURITY CLASS. *(of this report)* UNCLASSIFIED 15a. DECLASSIFICATION DOWNGRADING SCHEDULE

16. DISTRIBUTION STATEMENT *(of this Report)*

Approved for public release; distribution unlimited.

17. DISTRIBUTION STATEMENT *(of the abstract entered in Block 20, if different from Report)*

18. SUPPLEMENTARY NOTES

19. KEY WORDS *(Continue on reverse side if necessary and identify by block number)*

Concrete	Finite Element Analysis	Kolsky Bar
Dynamic Loads	Fracture	Materials Testing
Dynamic Properties	Impact	Rate Effects
Dynamic Testing	Hopkinson Bar	Reinforced Concrete Structures

20. ABSTRACT *(Continue on reverse side if necessary and identify by block number)*

This report describes the first-year activity of a three-year research program whose objectives are to (1) Develop a loading function for close proximity explosions, (2) Determine dynamic strength properties for selected types of concrete, (3) Incorportate the strength properties so determined into a localized failure criterion for reinforced concrete, (4) Use a structural analysis elastic/plastic finite element computer program to determine localized response for a concrete/steel finite element mesh,

(continued on back)

DD FORM 1 JAN 73 1473 EDITION OF 1 NOV 65 IS OBSOLETE UNCLASSIFIED

Block 20 (continued)

and (5) Combine all of these into a simple structural analysis program to determine response of underground structures to localized impulsive loads.

A new Kolsky Bar System (Split Hopkinson's Bar) is being built to test concrete specimens up to 3 inches in diameter. A pilot program testing 0.75-inch diameter specimens in an existing Kolsky Bar System has shown a linear dependence of the unconfined compressive strength of mortar on the strain rate at the maximum stress. The pilot program has been useful for guiding the design of the new larger system.

PREFACE

This is the first annual technical report on a planned three-year program of research sponsored by the U.S. Air Force Office of Scientific Research, Directorate of Aerospace Sciences, Bldg. 410, Bolling Air Force Base, D.C. 20332. Program Manager for the Air Force is Lt. Col. Lawrence D. Hokanson.

This annual report describes the technical effort during the period from 1 December 1982 through 30 November 1983.

The contractor is the University of Florida, Division of Sponosred Research, 219 Grinter Hall, Gainesville, Florida 32611. The research was performed by personnel of the Department of Engineering Sciences, University of Florida, Gainesville, Florida 32611 at the Gainesville campus of the university and at the University of Florida Graduate Center, Box 1918, Eglin Air Force Base, Florida 32542-0918. Co-Principal Investigators are Professor Lawrence E. Malvern at the Gainesville campus and Professor C. Allen Ross at the Eglin graduate center.

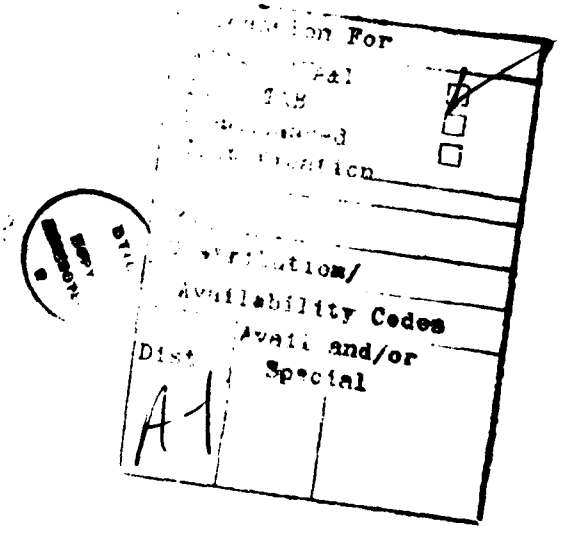

TABLE OF CONTENTS

LIST OF FIGURES

SECTION I

INTRODUCTION

A better understanding of the dynamic response of concrete and concrete structures to impulsive loadings is urgently needed as a foundation on which to base both designs for adequate protective structures and plans for munitions that can defeat protective structures. This fundamental research program investigates three major areas in order to contribute to a better understanding of the dynamic response. These three areas are (1) determination of the loads applied to a structure by a close-in conventional explosion, (2) strength properties of concrete at the high loading rates induced in a structure by a close-in conventional explosion, and (3) localized dynamic structural failure criteria.

A two-part investigation is addressed to these areas. Task I is an extension of previous studies at the University of Florida on structural response, while Task II addresses the material response by developing a new test facility to measure the compressive stress-strain response of concrete in the strain-rate range from 1 sec^{-1} to 1000 sec^{-1} and modeling the dynamic behavior. The two tasks are being pursued concurrently in a three-year program. This report summarizes the status of the program at the end of the first year.

The objectives of Task I are to:

1. Search literature and consult with other agencies in order to develop a loading function for the loads on structures resulting from cylindrical charges of arbitrary orientation,
2. Use a structural analysis elastic/plastic finite element computer program to determine early time localized response for a concrete/steel finite element mesh,

3. Search literature for dynamic localized failure criteria and possibibly develop a new criterion,
4. Obtain better estimates of dynamic properties of concrete from the results of Task II of this program, and
5. Combine all the above into a simple structural analysis program to determine response of underground structures to intense impulsive loads.

The research on Task I is directed by Prof. C.A. Ross. Current status of this research is reported in Section II.

The over-all objective of Task II is to develop representations for the dynamic response of concrete that can be incorporated into structural codes. Since very little experimental information is available on the material response at strain rates above about 5 sec^{-1}, a new test facility is being built for dynamic compressive testing at strain rates up to 1000 sec^{-1}. An existing Kolsky Apparatus (split Hopkinson's bar) with 3/4-inch diameter specimens is being used to test mortar with sand particles of maximum diameter 2.36 mm (1/8 the specimen diameter). For concrete with larger aggregate a new Kolsky Apparatus is being built to accomodate specimens up to 3 inches in diameter. The testing program on mortar was undertaken mainly for guidance in planning the new facility for concrete.

The design of the new system is almost complete, and construction of it is well under way, somewhat ahead of schedule. When it is completed, it will be a unique facility for studying the dynamic strength of concrete. Test results obtained with it will be used to guide the formulation of representations of the dynamic response of concrete in the range of strain rates important for structural response.

Section III reports the status of the research on Task II under the direction of Prof. L.E. Malvern. The research on Task II has been divided into three phases with considerable overlap in time between the phases Phase A, the testing of mortar with the existing system, is behind schedule, but some important results have been obtained, showing a linear strain-rate dependence of the unconfined compressive stength of the mortar up to strain-rates of the order of 800 sec^{-1}. This is a stronger rate dependence than had been expected, and, if the stronger dependence is verified also in larger grained concrete with the new testing facility, it will have a significant effect on modeling the dynamic structural response.

Section IV of this report lists some details of personnel involved in the research and interactions with other investigators in the field and closes with a brief indication of future plans for the program.

SECTION II

TASK I: FINITE ELEMENT CALCULATIONS, LOADING FUNCTION MODEL AND LOCALIZED DYNAMIC SHEAR FAILURE MODEL

2.1 Introduction

The proposed research under Task I contains three parts: 1) literature search and a loading function model, 2) finite element calculations and 3) localized shear failure model. The major portion of the work has been concentrated in the area of finite element calculations with minor emphasis on the literature search and localized shear failure model. The main reason for increased emphasis on the finite element portion is related to problems that arose in the process of placing the computer code NONSAP-C[1] in the computing system at Eglin AFB. Within the contract period a change in computer language from FORTRAN 4 to FORTRAN 5 and a change in computer types from a CYBERNET to VAX was required due to changes in the Eglin computing center. These changes required considerable time which ultimately reduced the time available for work on the problem of assessing the code for response of reinforced concrete structures.

2.2 Literature Search and Localized Shear Failure

The literature search is a continuous process and several documents have been reviewed concerning response of concrete material and structures. Those recent documents which are considered noteworthy to this phase of the contract are listed in Section 2.4 of this report.

The literature is practically void of information concerning pressure loadings from cylindrical explosives and discussion of localized shear failures. Reference 2 which gives details of experimental tests of cylindrical explosions in soils is the most recent work in the area of cylindrical explosives in soils but, due to the complicated presentations of the results and questions concerning the validity of some of the tests, the work is being reexamined. Reference 3, a rather voluminious book on The Dynamics of Explosion gives an empirical expression for over pressures from cylindrical charges in soil but it is only good for the experimental data from which it was taken as there is no variable to accommodate changes in explosive weight. However, Reference 3 is highly recommended as considerable discussion of effects of explosions are presented.

Current work in the area of dynamic shear failures is very limited, however some very good experiments (unpublished as yet) were conducted by US Army Waterways Experiment Station on shear failure of buried slabs due to intense uniform impulsive loads. These experiments are being studied for failure mechanisms which might be incorporated into analyses involving localized loadings. Two papers (pp. 95 - 103 of Reference 4) concerned with experiments and analyses of shear response in plain concrete are also being examined.

In additon to the work described in the following section some calculations involving a computer program ABAQUS (a proprietory program from Cybernet Services) is being planned in cooperation with the Air Force Engineering Services Center at Tyndall AFB, Florida. Identical problems are to be run on NONSAP-C and ABAQUS and analytical results will be available for comparisons.

2.3 Finite Element Calculation

In an effort to find a computer program that will predict response of reinforced concrete structures to localized loading, the computer code NONSAP-C[1] was obtained from the Los Alamos Scientific Laboratory, Los Alamos, New Mexico. This code has dynamic three dimensional capability with nonlinear finite elements with which the effect of both material and geometric nonlinearities are applied in the formation of the stiffness and stress recovery matrices. Three constitutive models for plain and reinforced concrete are available for use with the nonlinear two and three dimensional finite elements. Specifically these three constitutive models are a) an elastic-plastic model, b) an orthotropic variable modulus model and c) a concrete creep model. In particular the orthotropic variable modulus model contains both a concrete fracture criterion and a method of reducing stiffnesses in directions normal to the cracks. The reinforcing elements for this material model are incorporated in a "smeared" element stiffness representation. The "smeared" orthotropic representation means that the steel/concrete composite is treated as a single orthotropic material and the material properties for a given direction are described by a rule of mixtures based on the relative areas of steel and concrete. An additional variable is included to account for the bond degradation across a crack in the concrete matrix. Concrete cracking is controlled by the crack criterion, and when cracking does occur a stiffness reduction is made for the direction normal to the crack. When cracking occurs the material properties are then based on the reinforcing steel which is assumed to have an elastic-work- hardening constitutive relation with elastic unloading and reloading.

The basic program was received without plot routines and the major work with this code has been the addition of plot routines. Several basic plot

routines were added to plot displacements of all nodal points or only those required. A great deal of time was spent in trying to display damage to the structure. In the regular operation the program prints out messages of cracks and values of direction cosines normal to the cracks for each integration point of the element. In an effort to display structural damage the direction cosines were plotted as vectors on the undeformed structure. However, these did not appear satisfactory. As an alternate to the plot of direction cosine vectors, a small equilateral triangular plane was plotted normal to the direction cosine vector at each integration point of the finite element where it is indicated a crack had occurred. For three dimensional elements these planes are plotted along with the undeformed three dimensional array.

As an example of the use of these plots reinforced concrete slabs with planform dimensions of 10x10m and thickness of 0.5m and 0.25m were loaded at the slab center. The load was applied as a uniform load over one element as shown in Figures 1 and 3. The slab was simply supported on all four sides and only half the slab was used in the analysis. A loading function used for the analysis of both slabs is given in Table I below.

TABLE I

Loading Function for Slabs

Point No.	Time, millisec	Pressure, MPa
1	0.00	0.0
2	0.05	50.0
3	1.00	5.0
4	5.00	0.0

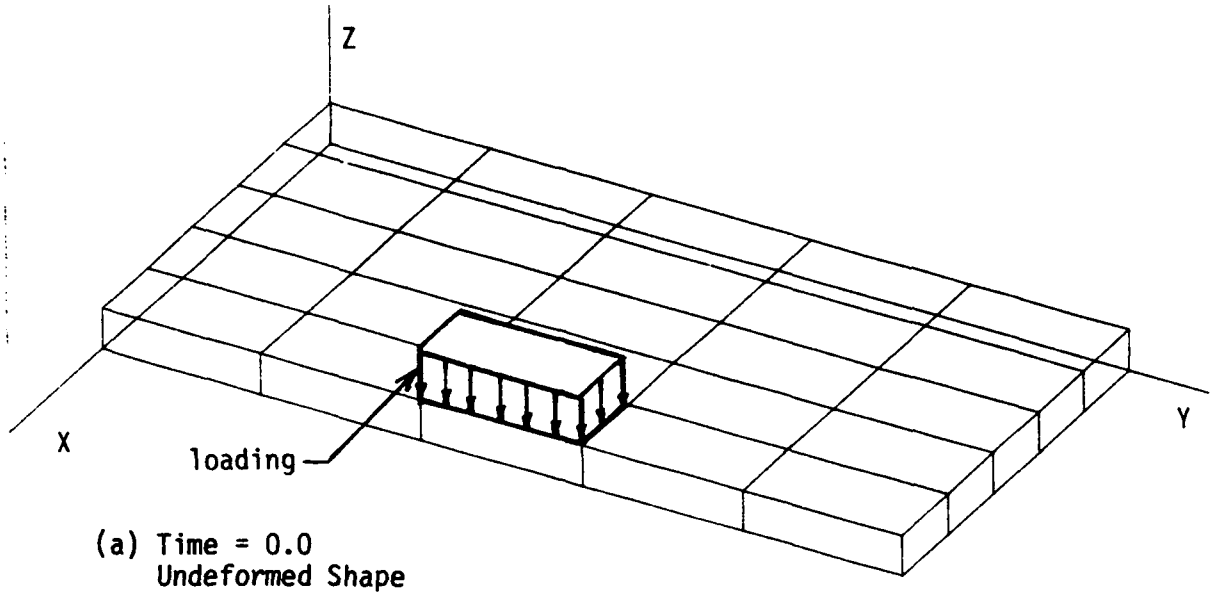

(a) Time = 0.0
Undeformed Shape

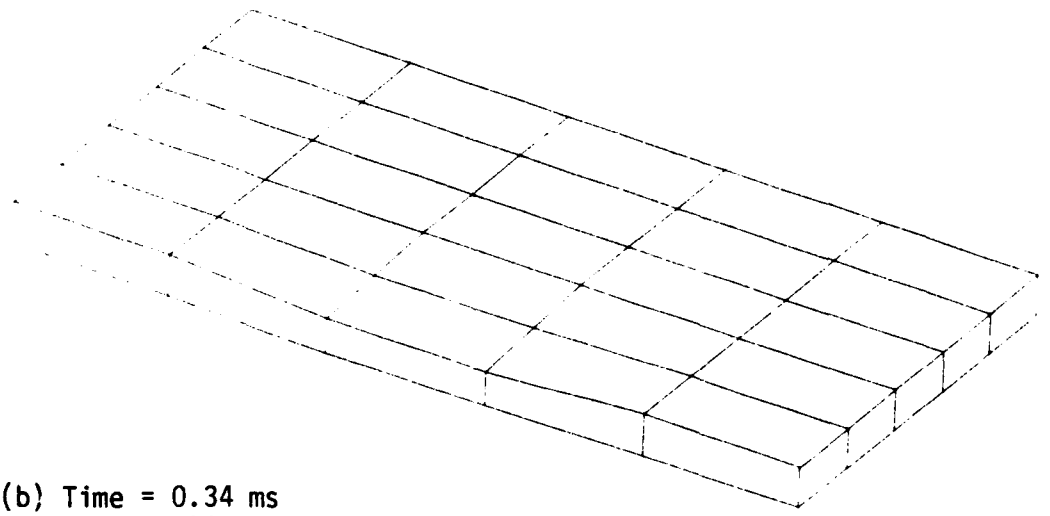

(b) Time = 0.34 ms
Maximum Displacement = 0.14 cm

Figure 1. Deformed shapes for reinforced concrete slabs. Loading shown in Figure 1a and given in Table 1. Dimensions: 10x10x0.5m. Due to symmetry only half of slab is shown.

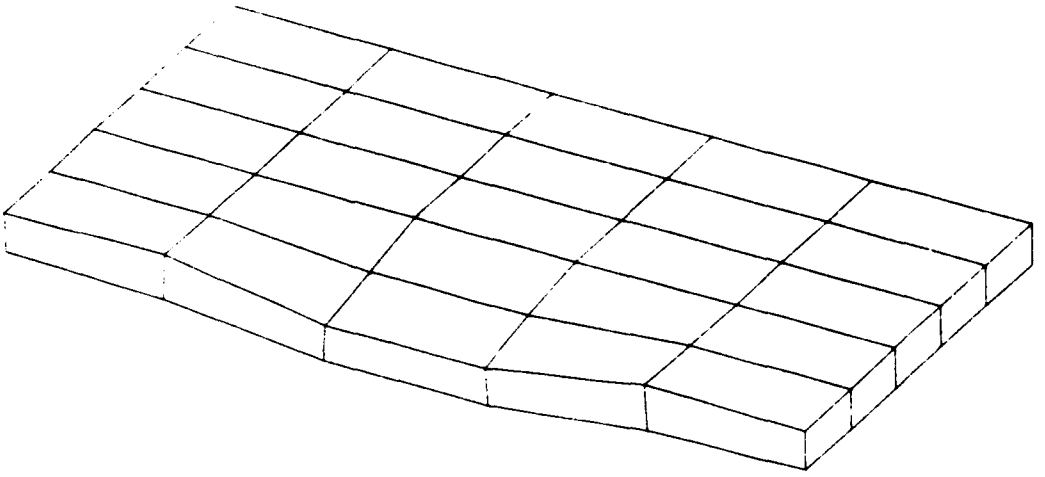

(a) Time = 0.68 ms
Maximum Displacement = 0.39 cm

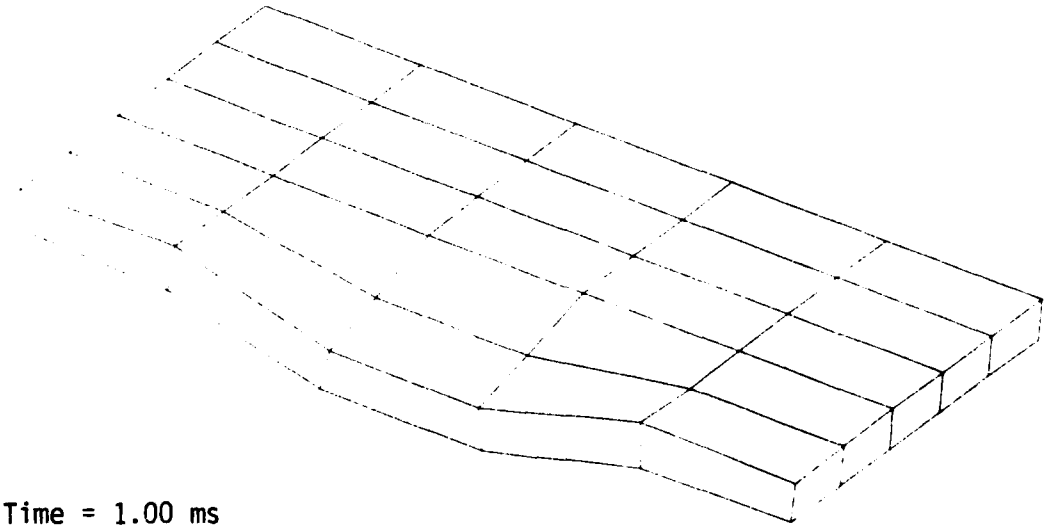

(b) Time = 1.00 ms
Maximum Displacement = 0.66 cm

Figure 2. Additional deformed shapes for reinforced concrete slab of Figure 1. Loading shown in Figure 1a and given in Table 1. Dimensions: 10x10x0.5m. Due to symmetry only half of slab is shown.

Both the slab and loading are generic and are used only in an attempt to demonstrate localized loading and damage in a reinforced concrete slab. The deformed shapes at given times for the 0.5m thick slab are shown in Figures 1 and 2 and the deformed shapes for the same times of the 0.25m thick slab are given in Figures 3 and 4. The displacement values for the thinner slab is about two to three times greater than the displacements of thicker slab and rather localized displacements are indicated in each slab for the localized loading. It is expected that the displacements would be further localized had the element size been reduced.

The cracked planes are shown in Figures 5 - 8. Figure 5a and 7a represent crack patterns where the first cracks appear for each slab thickness. The other Figures correspond to the same times as given for the deformed shapes of Figures 1B, 2, 3B and 4. Initial cracking for the model, Figures 5a and 7a, show cracking occurred at two opposite edges of the slab. These cracked planes lie almost parallel to the x-y plane and are a result of edge effects due to the symmetry condition that is imposed on the bottom nodes at the center line of symmetry. The code indicates that all the principal stresses are tensile for the two edge elements but for the internal elements the cracking is a result of one low tensile principal stress with reasonably high compressive stresses on the two orthogonal principal stress planes. This combination may cause failure on planes where the stresses are less than the uniaxial tensile failure stress.

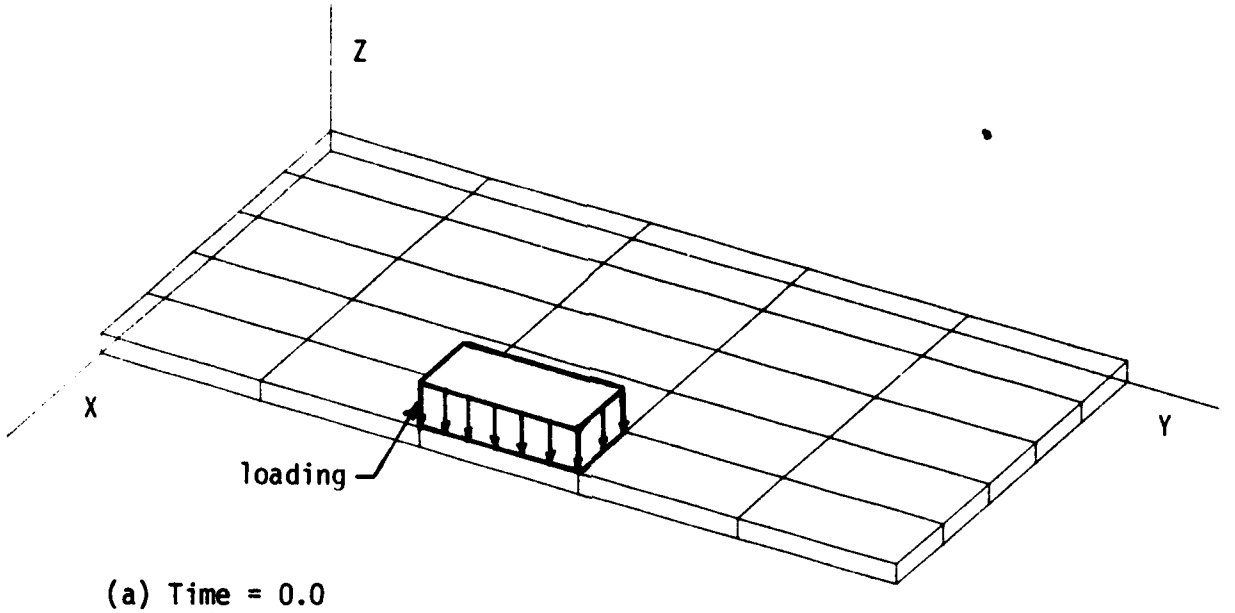

(a) Time = 0.0
Undeformed Shape

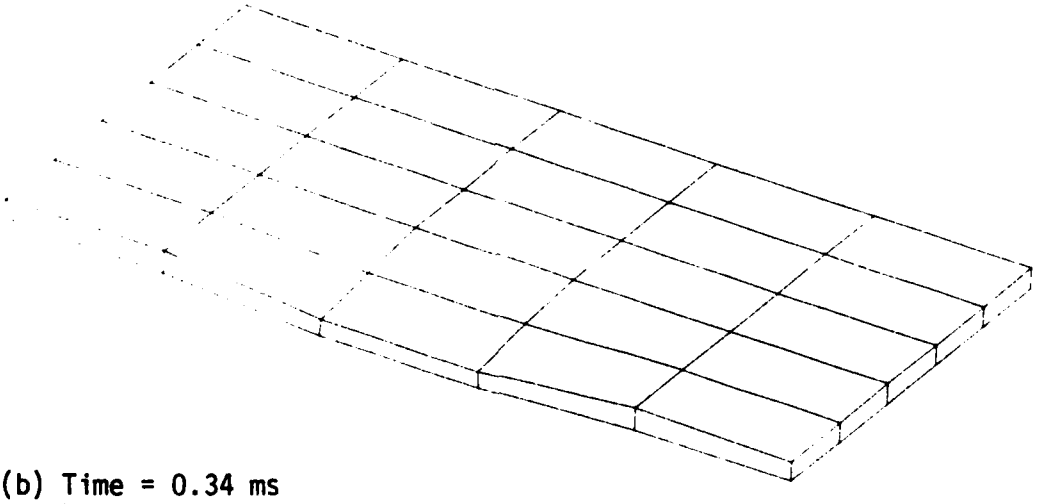

(b) Time = 0.34 ms
Maximum Displacement = 0.22 cm

Figure 3. Deformed shapes for reinforced concrete slab. Loading shown in Figure 3a and given in Table 1. Dimensions: 10x10x0.25m. Due to symmetry only half of slab is shown.

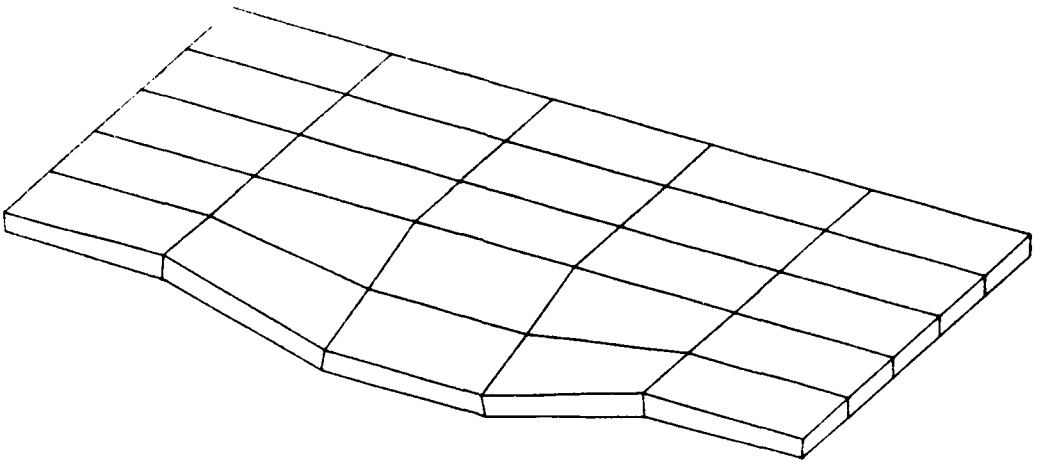

(a) Time = 0.68 ms
Maximum Displacement = 0.73 cm

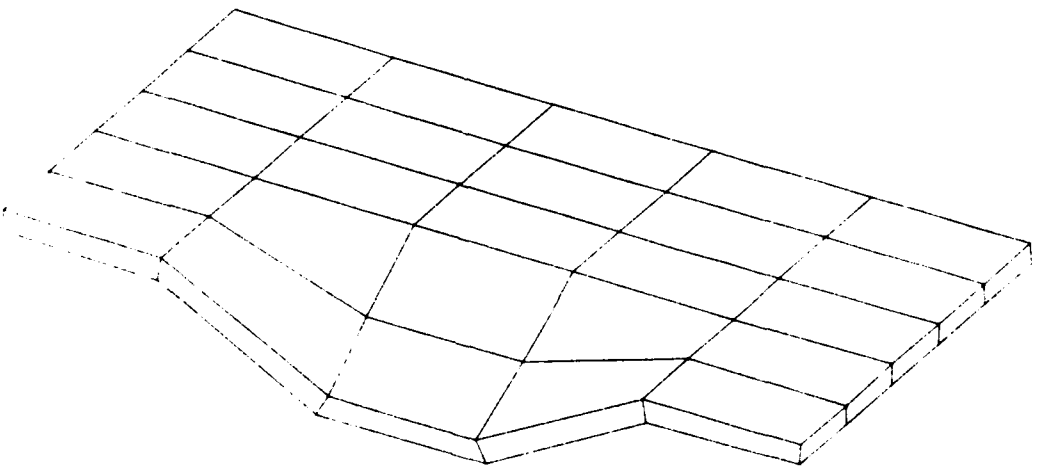

(b) Time = 1.00 ms
Maximum Displacement = 1.39 cm

Figure 4. Additional deformed shapes of reinforced concrete slab of Figure 3. Loading shown in Figure 3a and given in Table 1. Dimensions: 10x10x0.25m. Due to symmetry only half of slab is shown.

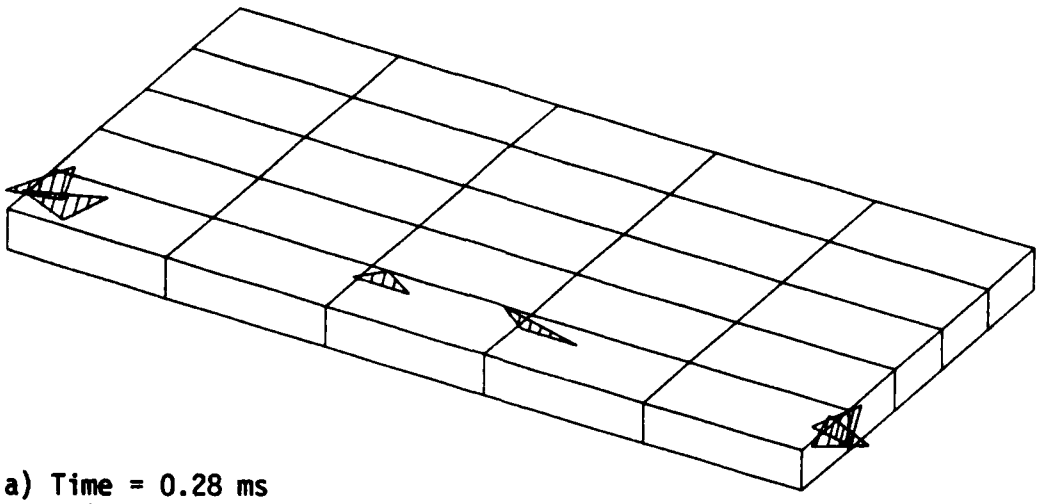

(a) Time = 0.28 ms
Initial Cracking

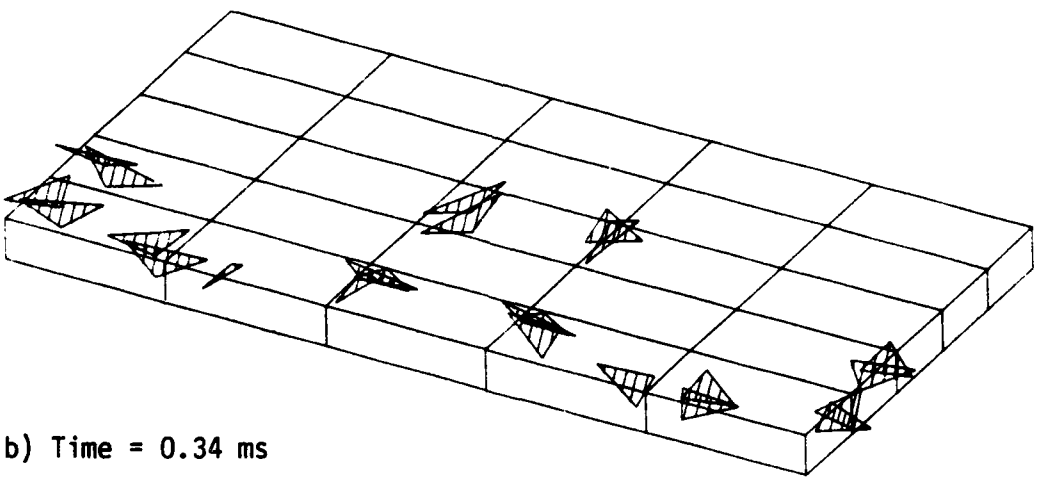

(b) Time = 0.34 ms

Figure 5. Crack patterns for slab given in Figure 1.

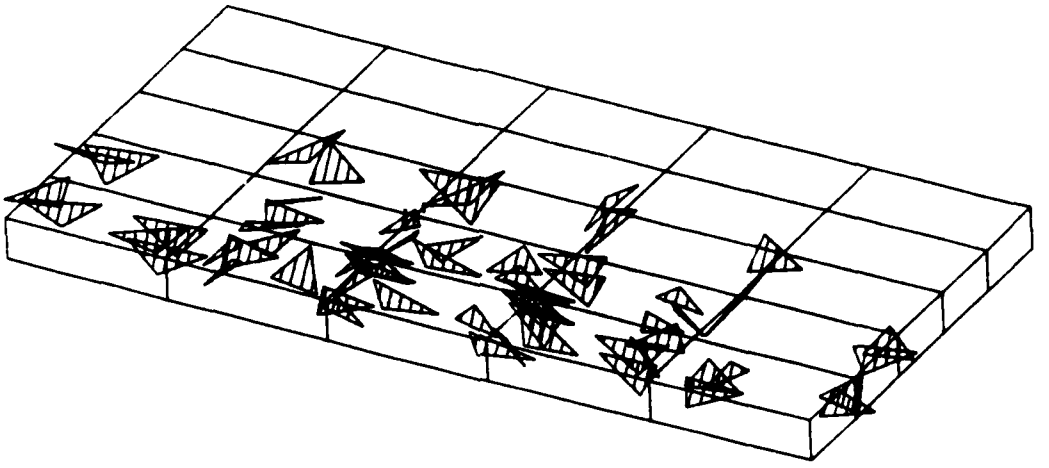

(a) Time = 0.68 ms

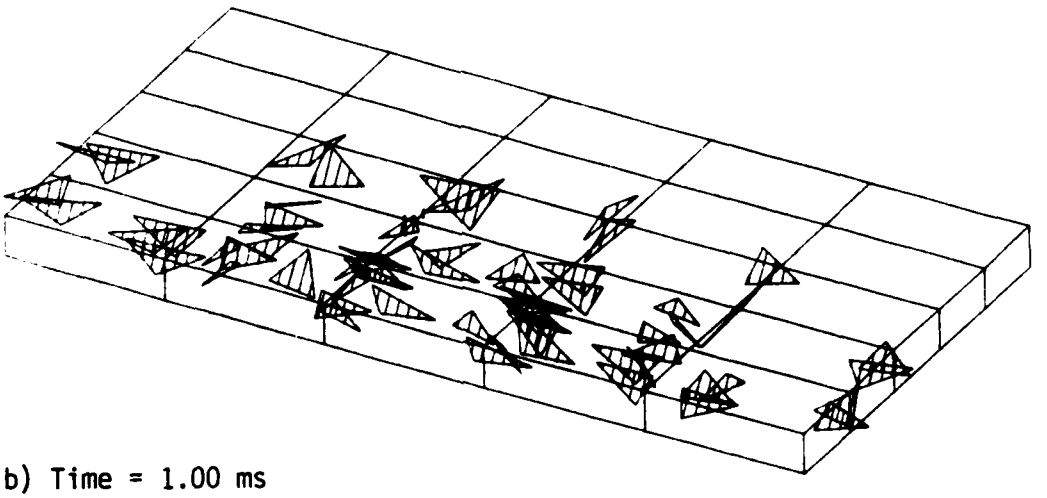

(b) Time = 1.00 ms

Figure 6. Crack patterns for slab given in Figure 2.

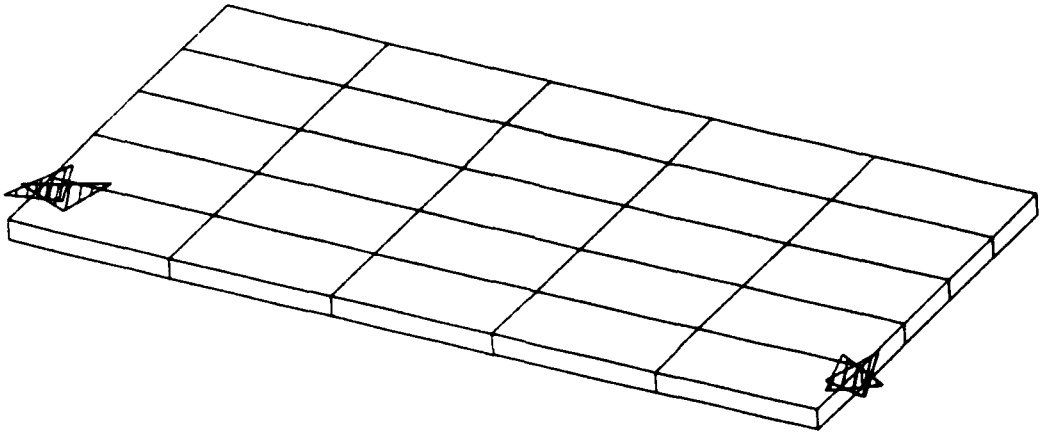

(a) Time = 0.16 ms
Initial Cracking

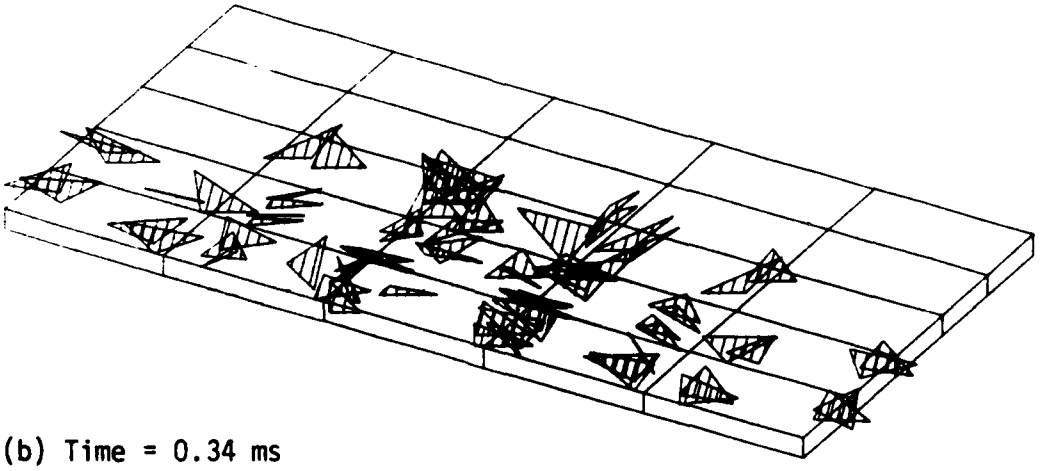

(b) Time = 0.34 ms

Figure 7. Crack patterns for slabs given in Figure 3.

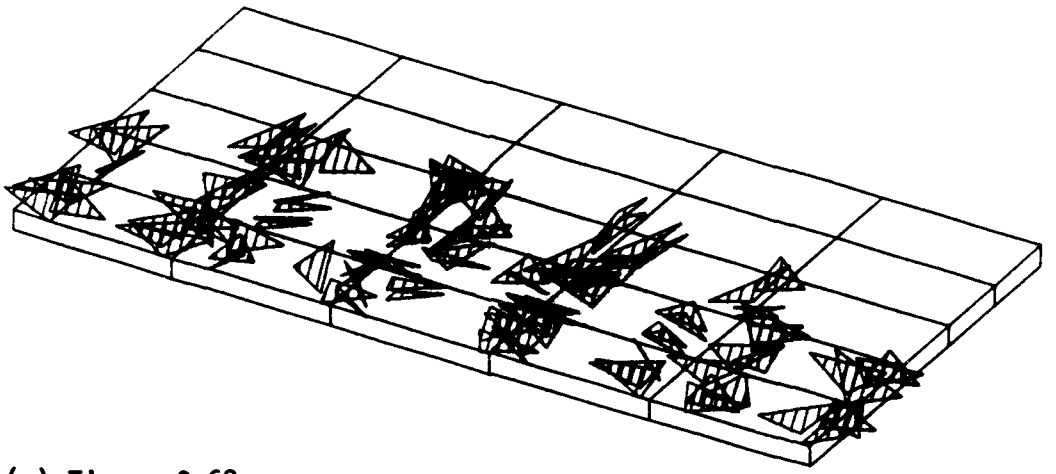

(a) Time = 0.68 ms

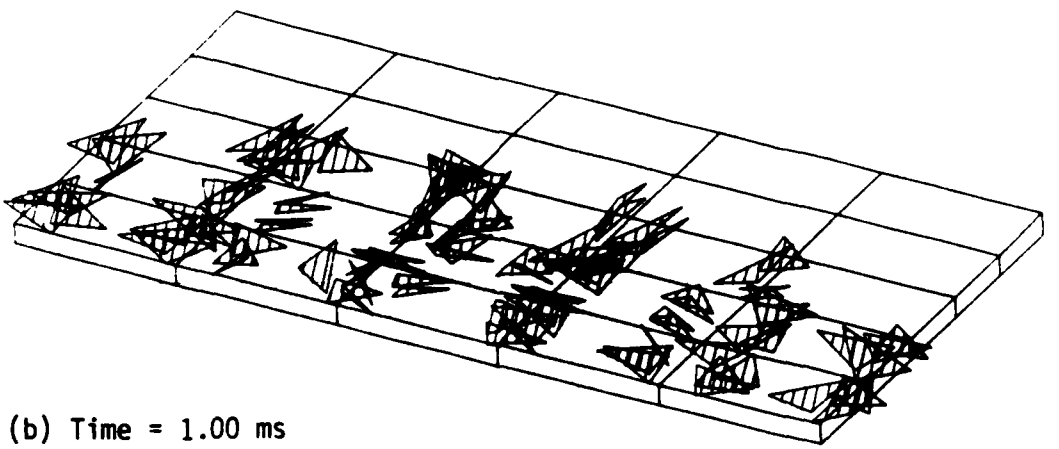

(b) Time = 1.00 ms

Figure 8. Crack patterns for slabs given in Figure 4.

2.4 References

1. Smith, P. D., and Anderson, C. A., "NONSAP-C: A Nonlinear Stress Analysis Program for Concrete Containments Under Static, Dynamic and Long-Term Loadings," NUREG/CR-0416, LA-7496-MS, Los Alamos Scientific Lab., Los Alamos, N.M., October 1978.

2. Westine, P. S., and Friesenhahn, G. J., "Ground Shock Loads from Buried Bombs and Ordnance Detonations," AFATL-TR-82-19, USAF Armament Lab., Eglin AFB, Florida, March 1982.

3. Henrych, J., The Dynamics of Explosion and Its Use, Elsevier Scientific Publ. Co., New York, N.Y., 1979.

4. Symposium Proceedings, "The Interaction of Non-Nuclear Munitions with Structures," USAF Academy, Colorado, May 1983, Vol. I: ADA 132116, Vol. II: ADA 132117.

SECTION III

TASK II - DYNAMIC STRENGTH OF CONCRETE

3.1 Introduction

The three-year effort under Task II is divided into three phases, with overlap between the phases. Phase A was initially planned for completion during the first year. It involves preparing and testing both unconfined and confined small compression specimens of mortar with an existing 3/4-inch diameter Split Hopkinson Pressure Bar system. This phase is behind schedule. There have been changes in graduate student assistant personnel and there were some delays in procuring the proper cement for the mortar specimens and in developing reproducible test procedures. No confined specimens have yet been tested, but good results have been obtained in unconfined tests.

These tests have indicated a type of strain-rate dependence quite different from that observed in metals. In metals, at least up to strain rates of about 10^3 per second, the rate dependence decreases at higher strain rates, so that an approximately logarithmic dependence on strain rate is observed. The tests on mortar suggest instead a linear dependence on strain rate when the dynamic strength is plotted versus the strain rate at the maximum stress. Preliminary tests had suggested that the rate dependence actually increased at higher rates, but further careful testing supports the linear plot up to the highest rates in these tests (about 800 sec^{-1}). The test equipment and procedures are reported in Section 3.2 and results summarized in Section 3.3. The principal motive for the test program on mortar was to gain experience and insight that would be helpful in designing the new bar in Phase B. Some of the insights gained will be mentioned in the following sections.

Phase B plans for the first year were to begin the design of a three-inch diameter Hopkinson Bar system and to procure components to assemble during the second year. This phase is ahead of schedule. Components have all been obtained except for a shock absorber, which has been ordered and should be delivered soon. Assembly has begun, and the first tests with the new bar should be made before the middle of the second year of the program. Some description of the new system is given in Section 3.4.

Phase C first-year plans called for beginning modeling studies that will continue through the three years. Preparation and testing of larger concrete specimens with the new system are included in Phase C in the second and third years. In addition to some empirical curve fitting, the modeling studies to date have included a literature search and attendance at conferences to promote acquaintance with other research and other investigators in the field, as summarized in Section 4.2.

3.2 Phase A - Mortar Tests Using Existing Experimental Facility

3.2.1 Test Equipment

The 3/4 inch (19 mm) diameter Split Hopkinson Bar at the University of Florida was used to determine unconfined compressive strength of mortar specimens at strain rates between about 50 sec^{-1} and 800 sec^{-1}. The specimens were cylinders of nominal length 10.16 mm and diameter 19 mm.

Figure 9 shows a schematic of the Hopkinson bar facility used for these experiments. The 23-inch long striker bar is propelled by a torsion-bar spring (not shown) to impact axially the incident pressure bar. Maximum loading time of approximately 230 microseconds is determined by the time required for the elastic compressive wave set up in the striker bar to return as an unloading tensile wave. The strain gages on the incident pressure bar are so positioned that this length of incident compressive pulse has passed

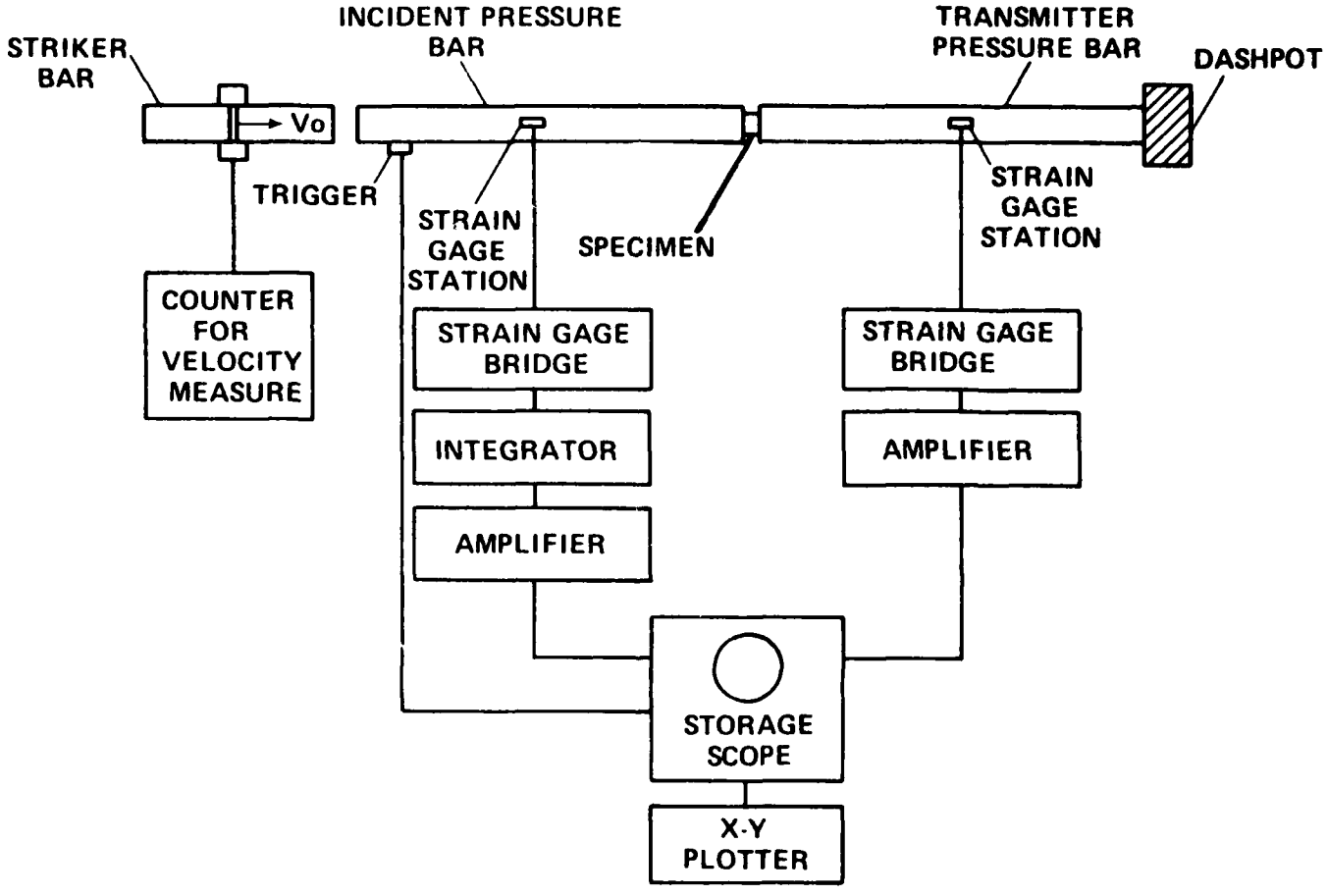

Figure 9. Schematic of Hopkinson Bar System Used for Mortar Tests.

the gage station and the trace has returned to zero, so that there is a dwell period before the reflected wave from the specimen end arrives, as is shown in the solid curve of Figure 10. The integrated reflected wave of Figure 11 is a measure of the average compressive strain along the length of the specimen, measured upward from the zero level established by the dwell period after the end of the incident pulse. The transmitted pulse is a measure of the specimen stress. Figure 12 shows the dynamic stress-strain curve for one of the small specimens. The signals of Figure 11 were recorded on a digital storage oscilloscope, and Figure 12 was plotted automatically by reading out the stress-time and integrated strain-time records of Figure 11 from the oscilloscope memory storage. The response for this specimen is almost linear up to the peak stress, and then drops off to a lower level as the specimen is crushed. Some other specimens show more bending over of the curve as the peak stress is approached.

Dynamic stress-strain curves obtained in this way give a good representation of material behavior when the specimen size and deformation rates are such that during the major part of the deformation the stress and strain are nearly uniform along the length of the specimen. Because of the short length of the specimens, many internal wave reflections between the ends of the specimen occur during the duration of the loading pulse, since the loading pulse length is long compared to the elastic wave transit time of about 3 or 4 microsec along the specimen. During the initial rapidly rising portions of the transmitted and reflected pulses the tansmitted pulse is delayed relative to the reflected pulse by the transit time through the specimen, as may be seen in Figure 10. Both the reflected pulse and the transmitted pulse, as recorded at the gage stations on the pressure bars, are of course seen later than they actually occur at the specimen interfaces

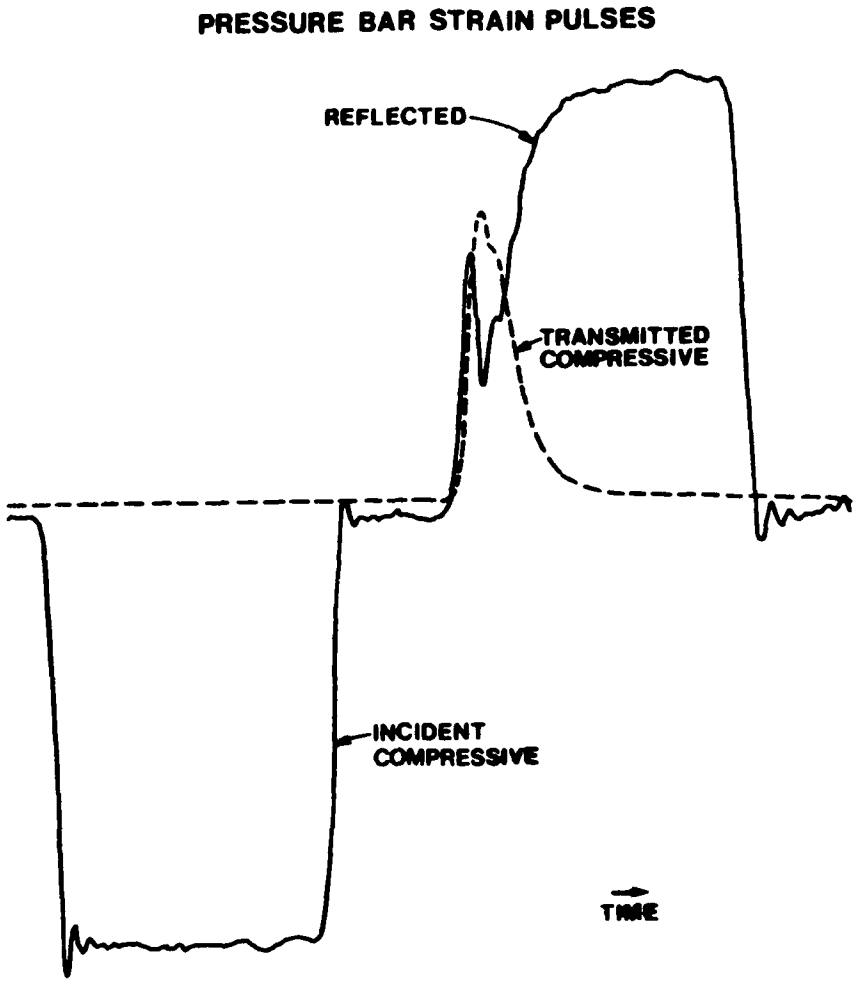

Figure 10. Strains Recorded on Incident Pressure Bar (Solid Curve) and Transmitter Pressure Bar (Dashed Curve).

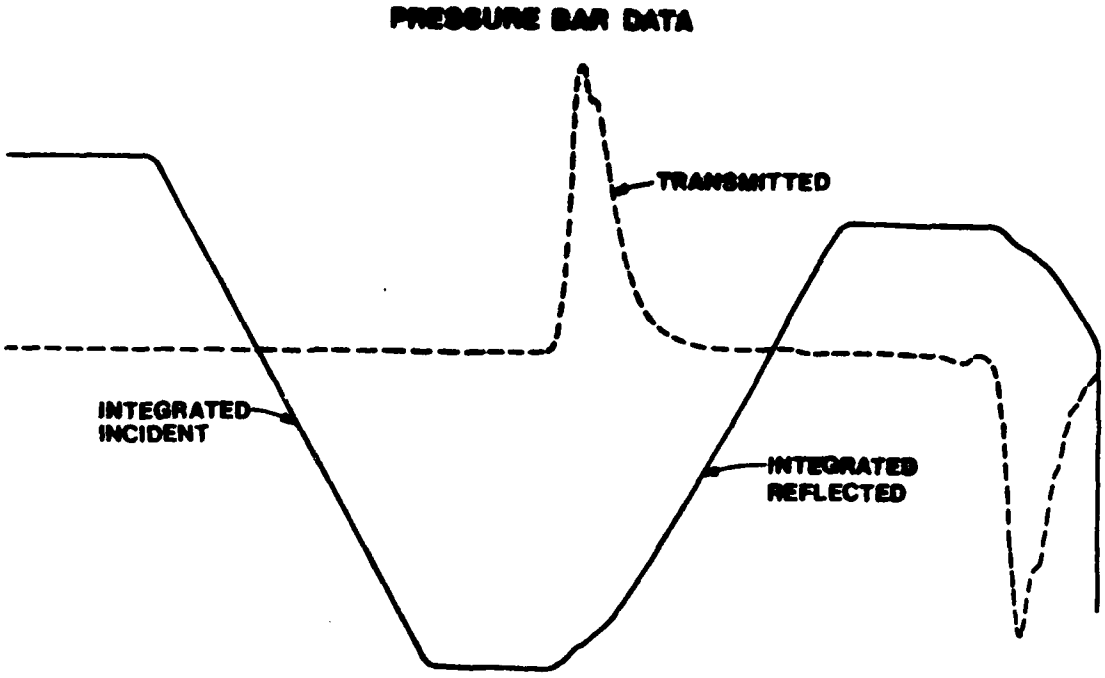

Figure 11. Transmitter Bar Signal Representing Specimen Stress, and Integrated Incident Bar Signals. (The integrated reflected pulse represents specimen strain.)

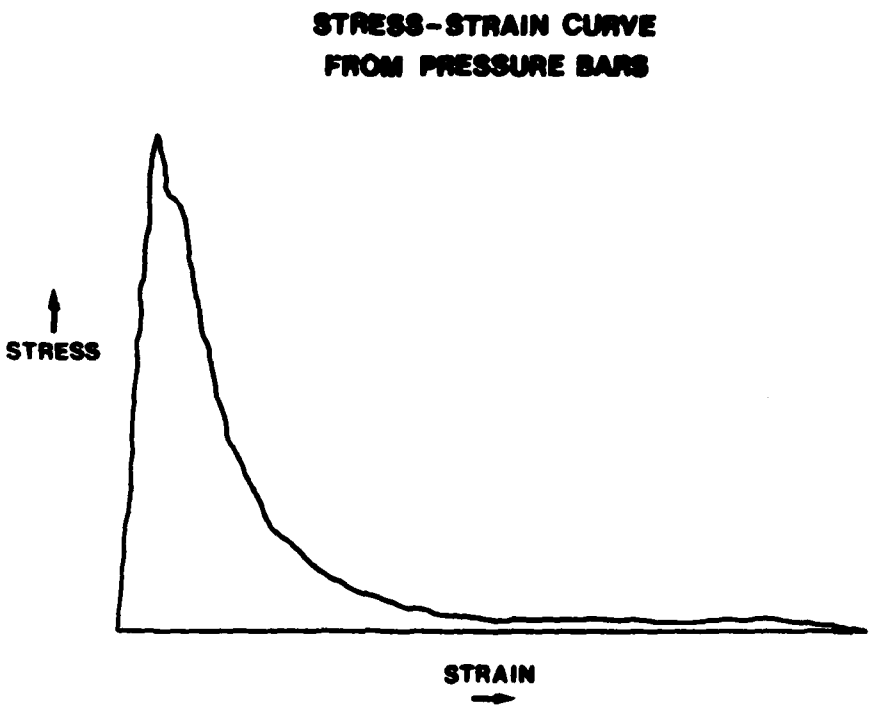

Figure 12. Stress-Strain Curve From Digital Recording of Pressure Bar Data.

because of the travel time in the pressure bars from the specimen interface to the gage station. It is important to have the two gages symmetrically placed. It is also important to have some dwell time between the end of the incident pulse and the beginning of the reflected pulse as recorded at the gage on the incident pressure bar. This permits the determination of the time zero for the beginning of the event at the specimen interface and also ensures that the shape of the rising portion of the reflected pulse is not distorted by the superimposed trailing part of the incident pulse.

The incident pulse length determined by the turnaround time in the striker bar appears in Figure 10 as the time from the initial incident pulse's downward movement to the end of the approximately flat maximum amplitude portion. The total duration of the incident pulse is longer than this by the time it takes for the pulse to return to zero. This unloading time is approximately equal to the initial rise time of the negative pulse. If the rise time is increased by tapering the striker bar or by cushioning the impact, the time from the beginning of the rise to the beginning of the fall is unchanged, for the same striker-bar length, but the increased fall time many increase the total duration of the record so much that the needed dwell time before the arrival of the reflected pulse is lost. This has been taken into account in the design of the new bar by providing longer incident and transmitter bars than initially planned. The reason for wishing to slow the pulse rise time while retaining the same impactor energy is to try to extend the Hopkinson bar measurements to a lower range of strain rates at specimen failure in order to bridge the intermediate strain-rate range between the static tests and the Hopkinson bar tests. Section 3.2.2 reviews the equations of the Hopkinson bar analysis. These are well known, but they are reproduced here to point out the approximations that are usually used, which may not be

good enough for the thicker concrete specimens to be used with the new 3-inch-diameter bar. It will also be shown how by using digital recording and a simple computer analysis of the data the range of validity of the results can be extended.

3.2.2 Hopkinson Bar Analysis

For a strain pulse propagating in the positive direction (away from the striker) in a pressure bar, elastic bar-wave theory furnishes the relationship

$$v = - c_o \varepsilon \tag{1}$$

between the particle velocity v and the strain ε (negative for compression), where c_o is the elastic bar-wave propagation speed. In the incident bar at the interface with the specimen the incident strain pulse ε_I gives velocity $-c_o \varepsilon_I$ and the reflected strain pulse ε_R propagating in the negative direction gives particle velocity $+c_o \varepsilon_R$, so that the net particle velocity v_I of the incident bar interface is

$$v_I = - c_o(\varepsilon_I - \varepsilon_R) \tag{2}$$

The transmitter bar interface particle velocity v_T is similarly found as

$$v_T = - c_o \varepsilon_T \tag{3}$$

where ε_T is the strain in the transmitted pulse. All these strains and particle velocities vary with time, while c_o is constant. The nominal strain rate $\dot{\varepsilon}_s$ in a specimen of initial length L_o is $(v_T - v_I)/L_o$ or

$$\dot{\varepsilon}_s = - \frac{c_o}{L_o} [\varepsilon_T - \varepsilon_I + \varepsilon_R] . \tag{4}$$

Equation (4) gives at any time the average strain rate along the specimen, (negative for compression) regardless of the specimen length, if the three recorded strain pulses at the gages are appropriately shifted in time (ε_I forward and the other two backward) before combining them. This can be accomplished by a simple computer program with digitally recorded data. In the usual analysis the further assumption is made that the stress in the

specimen is essentially uniform along the specimen length; then the same force acts on each pressure bar interface so that

$$EA(\varepsilon_I+\varepsilon_R) = EA\varepsilon_T \tag{5}$$

where E and A are the elastic modulus and cross-section area of the pressure bars.

This implies that

$$\varepsilon_I + \varepsilon_R = \varepsilon_T \, , \tag{6}$$

so that Equation (3) takes the simpler form

$$\dot{\varepsilon}_s = -\frac{2c_o}{L_o}\varepsilon_R \tag{7}$$

which has been used in almost all applications, including those reported in the following section for the small mortar specimens. Equation (7) is the basis of the statement in the preceding section that the integrated reflected strain pulse of Figure 11 is a measure of the average strain ε_s in the specimen. If the assumption of Equation (5) is not valid, then Equation (4) can be integrated instead of Equation (7). This will require a simple digital computer analysis because of the different time shifts between ε_I and the other pulses.

When the simpler Equation (7) can be used, the integration can be performed with an integrating operational amplifier in the recording circuit as was done to obtain the integrated trace of Figure 11. Then, with appropriate scaling, the reflected pulse of Figure 10 represents specimen strain rate, the transmitted pulse of Figures 10 and 11 represents specimen stress and the integrated reflected pulse represents the specimen strain, all plotted versus time as stated in Section 2.2.1. They can be read out point by point from the memory of the digital storge oscilloscope. They can also be replotted as stress versus strain on the digital oscilloscope display and then copied by an xy-plotter as in Figure 12.

When the assumption of Equation (5) is no longer valid, the computer routine mentioned earlier can be used to give average specimen strain. The specimen stress at the transmitter bar interface, σ_{sT}, will still be given by

$$\sigma_{sT} = E(A/A_s)\varepsilon_T \tag{8}$$

while the specimen stress at the incident bar interface, σ_{sI}, is given by

$$\sigma_{sI} = E(A/A_s)(\varepsilon_I+\varepsilon_R) \tag{9}$$

where A_s is the cross section area of the specimen, which should be less than or equal to the pressure bar cross section area A, and E is the pressure bar elastic modulus. An estimate of the average stress along the specimen length is then given by

$$(\sigma_s)_{Av} = \frac{1}{2}(\sigma_{sI}+\sigma_{sT}) \tag{10}$$

while an error estimate for the stress difference from the average is given by $\frac{1}{2}|\sigma_{sI} - \sigma_{sT}|$.

3.3 Mortar Tests

3.3.1 Specimens

The mortar specifications summarized in Table II were adopted after some trials with different mixes.

TABLE II

MORTAR SPECIFICATIONS

Cement: Portland Type I.

Aggregate: Sand conforming to ASTM C33 grain size

D_{max} = 2.36 mm D_{50} = 0.33 mm C_u = 2.11

Mix: (by weight) water/sand/cement = 0.55/2.5/1.0

Water: Tap water

Only sand passing U.S. standard sieve size No. 8, that is with diameter less than 2.36 mm, was retained; 50 percent was finer than 0.33 mm diameter and the coefficient of uniformity $C_u = D_{60}/D_{10}$ was 2.11.

The cement and sand are weighed separately and mixed by a rotary mixer for 3 minutes. Approximately half the water is slowly poured into the bowl and mixed for three minutes. A typical batch size was 1.43 kg water, 6.5 kg sand, and 2.6 kg cement. During this preliminary mixing the bowl is covered to prevent escape of particles. The rest of the water is then added and mixed for another 3 minutes.

The split PVC molds are prepared by lightly oiling the inside surfaces and placing silicone sealant along the joint edges. The halves are placed together and held with hose clamps. Molds are filled in a vertical position and then placed in a horizontal position for 24 hours.

Several different sizes and types of molds have been used. A careful pouring and tamping procedure with a rod is followed to promote uniformity in each specimen and from batch to batch. Table III shows most recent guidelines.

Table III

GUIDELINES FOR FILLING MOLDS

MOLD TYPE	SIZE Dia x Length (inches)	NUMBER OF LAYERS	RODDINGS PER LAYER
PVC	0.75 X 4	4	25
Steel	0.75 X 2	2	25
Split PVC	0.75 x 18	8	25
Split PVC	1.5 x 20	8	25
Cardboard	3 x 6	3	25

After each layer is rodded, the sides of the mold are lightly rapped to remove any trapped air. The 3x6 inch cardboard molds are vibrated on the bottom and sides with a pin vibrator for about 20 seconds per layer.

All PVC molds are sealed ovenight with rubber stoppers. After 24 hours the bars are removed from the molds and cured for 27 days in a wet room.

The nominally 0.4-inch-long dynamic compression test specimens are cut from the 3/4-inch-diameter mortar bars with a diamond saw. The bars are wieghed before cutting in order to determine the density, and each specimen is carefully measured with a micrometer after cutting.

Sulfur end caps are added to the 3x6 inch specimens, which are used for determination of the standard ASTM static strength f'_c. These tests are run on a Tinius Olsen Super L 400 kip testing machine in the Civil Engineering laboratory. For a more direct indication of rate effects, specimens nominally of 0.75-inch diameter and 1.5-inch length have been tested with an MTS elctrohydraulic testing machine in the Engineering Sciences laboratory.

3.3.2 Results of Dynamic Compression Tests of Mortar

The pilot program on dynamic compression testing of mortar used the existing 3/4-inch diameter split Hopkinson bar system described in Section 3.2. Dynamic tests were made on cylindrical specimens nominally 3/4 inch in diameter and 0.4 inch thick. The average strength in static compression test results from small specimens with the same diameter and 1.5-inch length at strain rates of the order of 10^{-3} sec^{-1} is plotted for comparison with the dynamic tests in Figure 13 (point appearing to be at zero strain rate). The average static compression results for standard 3x6 inch cylinders tested at nominal strain rates of the order of 10^{-4} sec^{-1} is labeled as f'_c in the legend of Figure 13.

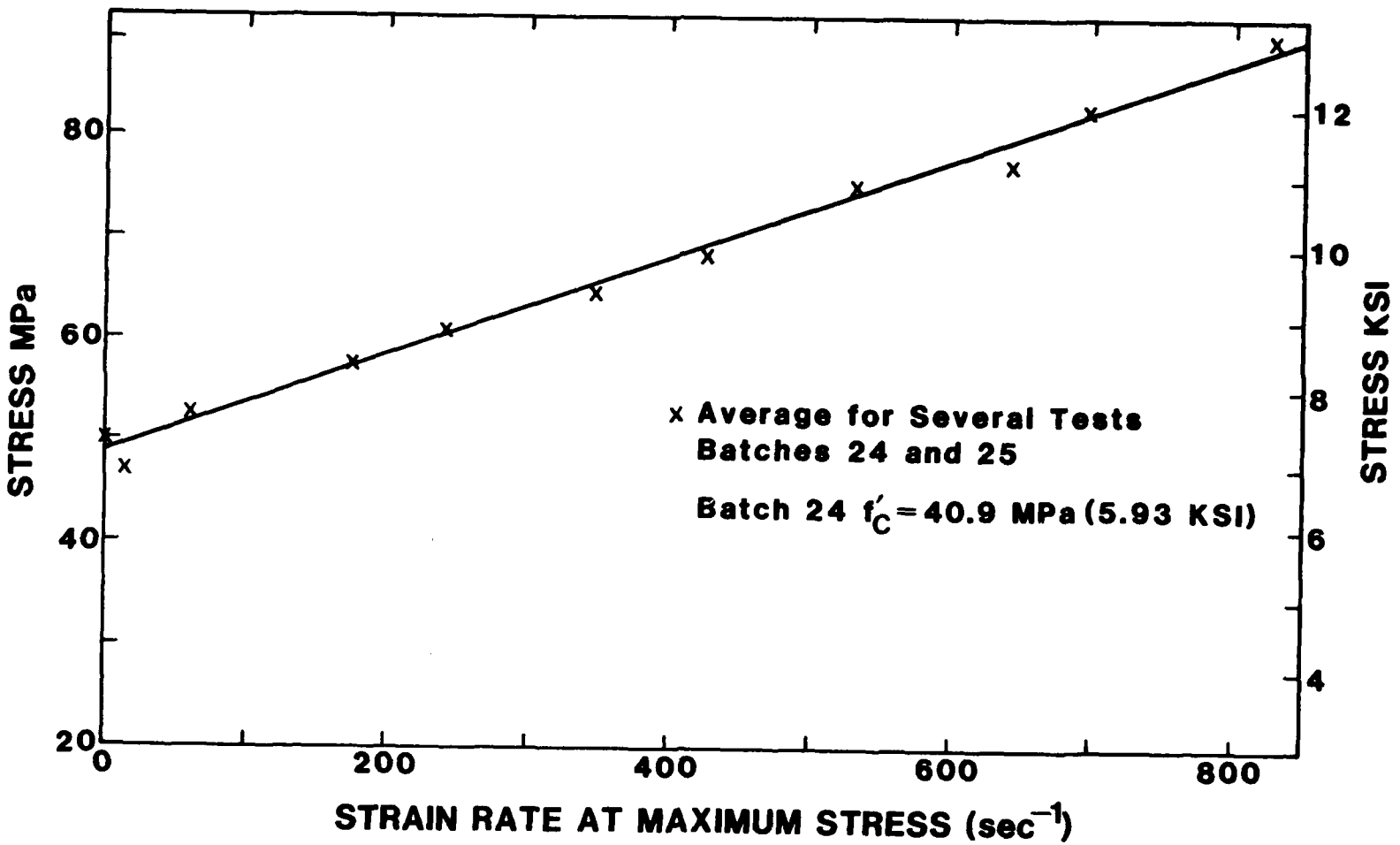

Figure 13. Maximum Stress Versus Strain Rate at Maximum Stress in Dynamic Compression Tests of Mortar.

Figure 13 shows a very good fit to a linear plot of maximum stress (at failure) versus the strain rate at maximum stress. Each plotted point is the average of 6 or 7 tests with the same striker-bar impact speed, except for the highest-speed case where only 3 tests were made.

The amount of scatter in these tests is shown in Figure 14 where each group of 6 or 7 points between adjacent dashed lines was obtained at the same impact speed (same drawback for the spring-driven striker bar). It is seen that there is scatter both in the strength values and in the strain rates at the maximum stress. Each plotted point in Figure 13 has strain rate equal to the arithmetic mean of the strain rates in the group of points at the same impact speed and ordinate equal to the mean strength of the group. Two batches prepared one week apart are included and marked by different symbols in Figure 14. The reproducibility between the two batches is quite good.

Despite the considerable scatter in each group the trend of maximum stress versus strain rate at maximum stress is quite clearly shown. A linear regression was used to fit the data by an equation of the form

$$\sigma = A + B(\dot{\varepsilon}/\dot{\varepsilon}_o) \qquad (11)$$

where $\dot{\varepsilon}_o$ is a reference strain rate, σ is the maximum stress and $\dot{\varepsilon}$ is the strain rate at the maximum stress. Table IV shows the coefficients A and B obtained for each fitted line. The value of R^2 is a measure of the quality of the fit (a value of R^2=1 would mean that every data point was on the line).

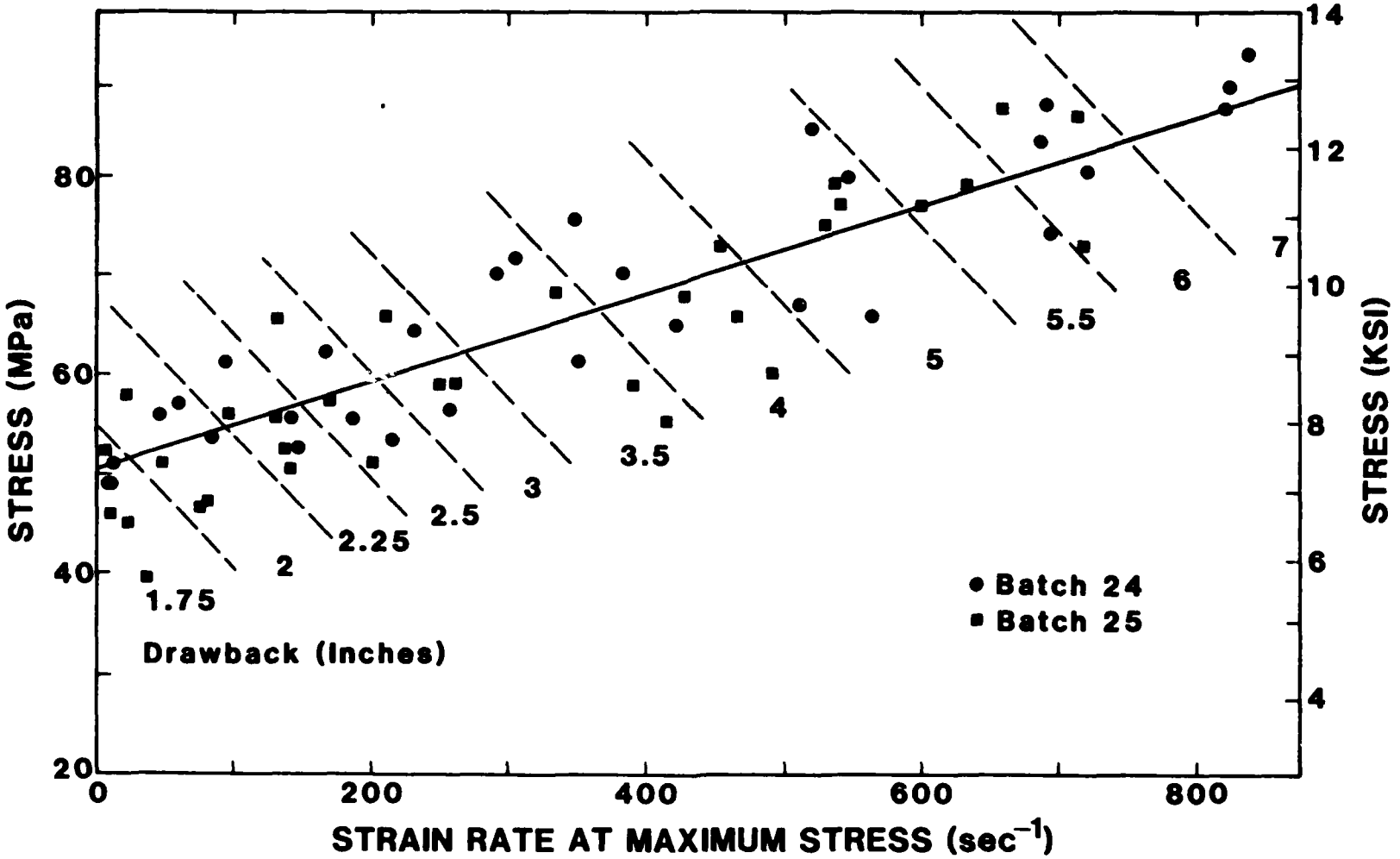

Figure 14. Scatter in Dynamic Compression Tests of Mortar. (All data points between two adjacent dashed lines were obtained at the same impact speed.)

TABLE IV

COEFFICIENTS A AND B FOR FITTING EQUATION (11) TO RESULTS OF FIGURES 13 and 14 WITH REFERENCE $\dot{\varepsilon}_o = 10^{-3}$ sec^{-1}.

($R^2 = 1$ would mean perfect fit.)

	(MPa)		(KSI)		
	A	B	A	B	R^2
Figure 13 (12 points)	48.8	47.9	7.08	6.94	0.992
Figure 14 (All points plus 3 static tests)	50.3	44.2	7.30	6.41	0.784

The nature of the scatter within each group in Figure 14 may seem surprising at first, with higher strengths appearing to occur at the lower strain rates for specimens all impacted at the same speed. This would be surprising if the specimens were identical, but there is an inherent scatter even in the static strength values. The stronger specimens in the group remain elastic to higher stress values, and this can result in insufficient impactor energy remaining to promote rapid deformation at failure. This is especially apparent in the group impacted at the lowest speed (1.75-inch drawback). Examination of the failed specimens in this low-speed group frequently revealed that only a few longitudinal cracks had been produced, while at the higher strain rates the specimen was pulverized. At still lower impact speeds the specimen appears to remain elastic, and the maximum stress obtained is limited by the available energy instead of specimen strength.

A different kind of dependence of stress on strain rate (possibly not linear) might well be obtained if instead of maximum stress versus strain rate at maximum stress, the plot had been of stress at a specified strain in the microcracking regime between the elastic regime and failure versus the strain

rate at the specified strain. This analysis has not been made as yet, but the stress, strain and strain rate data for several specimens have all been stored digitally on floppy disks. A computer program is in preparation to make the analysis at prefailure strains without the tedious point-by-point manual read-out of the data.

The maximum strength data is what is currently input into structural analysis codes for concrete. In the present state of the art, the static values are used, possibly multiplied by a dynamic correction factor to account in some way for the average strain rate during the event.

The tests reported above are only the most recent two series of tests, where both the material and the testing procedure were so well controlled that a good reproducibility was obtained between the results of Batch 24 and Batch 25. Some reasonably good results had been achieved in earlier tests, but because the strength is so dependent on the compaction and cure procedures it is difficult to obtain reproducibility between specimens prepared at different times. Agreement in the measured densities and elastic wave speeds were found to be fairly good predictors that the dynamic strengths would be reproducible, but both the static and dynamic strengths of these small mortar specimens are highly sensitive to the amount of air drying time between the end of the 28 day moist cure and actual testing. Delays were sometimes caused by waiting to get the specimens cut or waiting to get the Hopkinson bar realigned, and this contributed to the lack of reproducibility.

3.3.3 Dynamic and Static Moduli

Elastic bar wave speeds c_o were measured on mortar bars of nominal 3/4-inch diameter and lengths from 13 to 16 inches by cementing a small accelerometer to one end of each bar and tapping the other end lightly with a

small hammer instrumented with a force transducer that was used to trigger the digital oscilloscope. Round-trip transit times were measured between successive arrivals of the leading edge of the pulse at the accelerometer. The dynamic elastic modulus E was then calculated by

$$E = \rho c_o^2 \quad . \tag{12}$$

This modulus is related to small-amplitude pulses propagating in an unloaded bar. Average density was 2980 kg/m^3. Values of c_o determined on seven bar specimens varied from 3730 m/s to 3940 m/s. Averages are listed in Table V at the end of this section.

Dynamic moduli were also calculated from ultrasonic wave speeds measured on short specimens like those used for the Hopkinson bar tests. The ultrasonic speeds were measured with a Panametrics Time Intervalometer System 5054, which applies a short broad-band pulse repetitively to a quartz transducer on one face of the specimen, which can be used both for sending the ultrasonic pulse and receiving reflections from the opposite face. A second receiving transducer is mounted on the opposite face, which records the arrival of the first pulse and of successive reflections back from the first face. Both the longitudinal wave speed c_1, and the shear wave speed c_2 were determined. For c_1, a pair of Panametrics V-106 transducers with half-power bandwidth 2.25/0.5 MHz were used. For c_2, Panametrics V-153 shear transducers with bandwidth 1.0/0.5 MHz were used.

A precisely controlled variable oscilloscope sweep speed was used to display and overlap two successive signals on two successive sweeps. The sweep repetition period is the time between the two signals. For the shear waves, the two signals overlapped were the first and second signals arriving at the receiving end of the specimen. For the longitudinal waves the two signals used were the first arrival at the receiving end and the first

reflection back to the sending end; these two signals are 180° out of phase, but it was easy to match the two pulses.

The moduli are then calculated by the following well-known equations of the theory of elasticity, where λ is the Lamé constant. and ρ is density.

$$\lambda + 2G = \rho c_1^2 \tag{13}$$

$$\text{Shear Modulus } G = \rho c_2^2 \tag{14}$$

$$\text{Elastic Modulus } E = \frac{G(3\lambda + 2G)}{\lambda + G} \tag{15}$$

$$\text{Poisson's Ratio } \nu = \frac{\lambda}{2(\lambda + G)} \tag{16}$$

TABLE V

WAVE SPEEDS AND ELASTIC CONSTANTS

FROM BAR-WAVE TESTS (7 specimens):

c_o = 3840 m/s (1.51×10^5 in/sec) ± 3 percent

E = 31 GPa (4.5×10^6 psi)

FROM ULTRASONIC TESTS (24 specimens)

c_1 = 4130 m/s (1.63×10^5 in/sec) ± 3 percent

c_2 = 2570 m/s (1.01×10^5 in/sec) ± 6 percent

λ = 8.0 GPa (1.16×10^6 psi)

G = 13.6 GPa (1.97×10^6 psi)

E = 32 GPa (4.6×10^6 psi)

ν = 0.18

Calculated $c_o = (E/\rho)^{1/2}$ = 3940 m/s

STATIC MODULUS (approximate):

E = 21 to 27 MPa (3 to 4 x 10^6 psi)

DENSITY

ρ = 2080 kg/m^3 ± 2 percent

Table V summarizes the results obtained with Batch 24 and 25. The estimate of the static modulus is based on approximate measurements with an extensometer on a 3/4-inch diameter specimen in the MTS testing machine.

3.4 Design of New Test Facility For Larger Specimens.

For concrete more like that in structures of interest, a larger aggregate size will be tested. This will require a larger specimen size in order to keep the aggregate small compared to the specimen. The proposed Phase B design called for a specimen size up to 3 inches in diameter and 1.5 to 3 inches long. The pressure-bar system was to have three-inch-diameter pressure bars.

In the preliminary design, a striker-bar length of 30 in, to produce a loading pulse length of about 300 microsec, was chosen. It will be propelled by a gas gun, which will permit convenient substitution of different length strikers.

With the 30-inch striker, an 80-inch incident bar would provide a dwell time of about 100 microsec between incident and reflected pulses at the middle of the bar. The final design increased the incident and transmitter bar lengths to 120 inches in order to preserve the 100 microsec dwell time even if the rise and fall times of the loading pulse were increased to 200 microsec by tapering the striker bar or by cushioning the impact, causing the total incident pulse length (loading pulse plus fall time) to increase to 500 microsec. This will permit a considerable flexibility in impactors used and is expected to make possible testing to failure at lower strain rates in the intermediate range between the highest rates attainable with an ordinary testing machine (of order 1 sec^{-1}) and the lowest rates previously attainable with the pressure bar system (50 to 100 sec^{-1}).

Impactor speeds up to 15 m/s (600 in/sec) should be sufficient for the dynamic compression tests planned. It may be noted that the maximum impactor speed to reach the dynamic strength of 92.4 MPa (13.4 KSI) at a strain rate of 835 sec^{-1} in Fig. 14 was 14.2 m/s (560 in/sec). Some similar tests on high-strength fine-grained concrete at the University of Florida in 1981 crushed the specimen at 182 MPa (26.4 KSI) with an impactor speed of 12 m/s (475 in/sec).

A gas gun for propelling the striker bar of the system has been built by Terra Tek, Inc. of Salt Lake City, tested at Terra Tek and delivered to the University of Florida. It is operated from a 2000 psi nitrogen bottle through a console providing pressure reducers and firing control. Its 30-inch, 61.3- pound, striker bar attains the speed of 15 m/s after traveling 24 inches in the barrel with a firing chamber pressure of only 375 psig. The firing chamber is designed for operating pressures up to 2000 psi, but has been proof tested only to 650 psi. The striker is guided in the barrel by Teflon bushings, which also provide a pressure seal until the rear end of the striker passes vent ports which release the pressure when the nose of the 30-inch striker bar reaches the muzzle.

The incident pressure bar will be mounted so that the striker bar impacts it in a position about two inches in front of the muzzle. The two 120-inch-long pressure bars, three inches in diameter, will be supported on pillow blocks mounted on a 12-inch-wide channel section 23 ft long, which serves as a table top supporting the pressure bar system. A welded steel structure will support the channel section. The structural steel has been obtained and cut, and welding operations will begin about February 1, 1984. The total length of the system, including the air gun will be 29 ft.

The pressure bars are ETD-150 ground and polished, cold finished steel bars comparable in analysis to 4140 steel. The yield strength is specified by the distributor as 152.5 KSI (1050 MPa) and the hardness as 36 Rockwell. The bars have been cut to length and the ends faced.

The preliminary design called for a momentum trap consisting of another bar of the same size as the striker bar to be placed at the far end of the transmitter bar. The idea was that it would fly off with all the imparted momentum, leaving the pressure bars in place. The momentum trap would be stopped by a shock absorber. A little analysis and experimentation with the existing small bar system showed, however, that when an inelastically deforming specimen is in place between the incident and transmitter bars only about one-fourth of the striker's momentum is transferred to the transmitter bar during the loading pulse. The incident bar continues in motion, and the whole system must be stopped by the shock absorber. The final design therefore omitted the momentum trap and placed only a short spacer between the shock absorber and the transmitter bar. Spacers of different lengths will provide for consistent positioning of specimens of different lengths without moving the shock absorber. A shock absorber has been ordered from Ace Controls, Inc. of Farmington, Michigan. Delivery is expected about February 1, 1984. It will be an Ace PCHA 1-1/2 x 6-1/2 inch shock absorber with 6.5-inch stroke with some modifications on the orifices to provide for higher speeds.

The strain-gage amplifier instrumentation for the system has been designed and components assembled. It will be essentially identical to a new system installed and tested on the existing pressure bar system this year. Provision will be made for direct calibration of the strain-gage system with gages on the pressure bars without depending on the impactor velocity

measurement, since the velocity measurement is the least precise measurement in the operation. The calibration will, however, be checked against the velocity measurement.

A new four-channel digital oscilloscope, purchased on a DoD Research instrumentation grant to the University of Florida has been delivered and will be used as a transient data recorder with the new bar system. It has a considerable amount of internal data analysis capability, including smoothing, integrating, time shifting and adding two signals. It will be connected to a microcomputer and/or to a computer terminal for further automated data analysis. This part of the system is still to be designed.

SECTION IV

PERSONNEL, INTERACTIONS, AND FUTURE PLANS

4.1 List of Professional Personnel Associated with the research.

Prof. L.E. Malvern

Prof. C.A. Ross, Co-Principal Investigators

Dr. D.A. Jenkins, Associate Engineer

Dr. H.W. Doddington, Engineer, Director of Engineering Sciences Instrumentation Staff

E. Jerome, Assistant in Engineering (Computer Analyst)

T. Tang, visiting Scholar in Engineering Sciences

R. Gupta, graduate student in Civil Engineering

J.P. Shoucair, graduate student in Civil Engineering

4.2 Interactions

A paper, "Dynamic Compressive Testing of Concrete and Mortar," by T. Tang and L.E. Malvern, is being prepared for submission to the ASCE Fifth Engineering Mechanics Division Specialty Conference to be held at the University of Wyoming, 1-3 August 1984.

Professor Ross was coordinator of an Air Force sponsored Symposium on the Interaction of Non-Nuclear Munitions with Structures, held at the Air Force Academy, 10-13 May 1983. This symposium brought together investigators not only from the United States, but also from The United Kingdom, The Federal Republic of Germany, The Netherlands, Sweden, Switzerland and Italy. Professor Malvern also participated in the symposium and was co-chairman of a session on Material Models.

Other conference participation by Professor Malvern included:

(1) Symposium on Nonlinear Numerical Analysis of Reinforced Concrete at the ASME annual meeting in Phoenix, 18 November 1982.

(2) ASCE Engineering Mechanics Specialty Conference at Purdue, 23-25 May 1983, which had technical sessions on Constitutive Modeling and Dynamic Response of Concrete, Inelastic Analysis, and Structural Behavior Under Extreme Over-Pressure and/or Ground Shock, and

(3) Invilted participation at IUTAM Symposium on Mechanics of Geomaterials: Rock, Concrete and Soils, Northwestern University, 11-15 September 1983.

Professor Ross has been actively involved in a research program on "Building Structure Vulnerability: Below Ground" sponsored by the U.S. Air Force Armament Laobratory.

4.3 Future Plans

During the second year of the Task I research two prinicpal items will be emphasized: (1) developing the loading function, and (2) incorporating into the finite element analysis some method of taking account of the strain-rate dependence. Some recent experimental studies at the U.S. Army Waterways Experiment Station will be used to check analytical formulations of the loading function. The finite element code will be modified so that it can monitor the strain rates predicted by the analysis and provide for updating the material property parameters to take account of the rates.

The Task II second year calls for completion of the new Kolsky apparatus and the beginning of testing of concrete with larger aggregate. The mortar studies will also be continued, and both unconfined specimens and steel-jacketed confined specimens will be tested. The preparation of jacketed

specimens should be easier with the larger 3-inch diameter system. A simple computer program will be developed for automated data analysis, as was suggested in Section 3.2.2, and the rate dependence of the stress-strain relationship in the microracking regime between the elastic range and the maximum stress will be examined.

Testing facilities for the lower part of the intermediate strain rate range between the highest rates attainable with an ordinary testing machine (of order 1 sec^{-1}) and the lowest rates attainable with the Kolsky bar system will be designed.

Modeling of the uniaxial rate dependence will be pursued, and existing (mainly rate-independent) multiaxial constitutive equations will be studied to determine how best to include rate effects in a practical three-dimensional calculation.